SLEEPJ, 2021, 1–15

doi: 10.1093/sleep/zsaa237
Advance Access Publication Date: 13 November 2020
Original Article

ORIGINAL ARTICLE

Altered circadian activity and sleep/wake rhythms in the stable tubule only polypeptide (STOP) null mouse model of schizophrenia

Samuel Deurveilher[1], Kristin Robin Ko[2], Brock St. C. Saumure[1], George S. Robertson[3,4], Benjamin Rusak[3,5] and Kazue Semba[1,3,5,*]

[1]Department of Medical Neuroscience, Dalhousie University, Halifax, NS, Canada [2]School of Biomedical Engineering, Dalhousie University, Halifax, NS, Canada [3]Department of Psychiatry, Dalhousie University, Halifax, NS, Canada [4]Department of Pharmacology, Dalhousie University, Halifax, NS, Canada [5]Department of Psychology & Neuroscience, Dalhousie University, Halifax, NS, Canada

*Corresponding author. Kazue Semba, Department of Medical Neuroscience, Dalhousie University, 5850 College Street, PO Box 15000, Halifax, Nova Scotia B3H 4R2, Canada. Email: k.semba@dal.ca.

Abstract

Sleep and circadian rhythm disruptions commonly occur in individuals with schizophrenia. Stable tubule only polypeptide (STOP) knockout (KO) mice show behavioral impairments resembling symptoms of schizophrenia. We previously reported that STOP KO mice slept less and had more fragmented sleep and waking than wild-type littermates under a light/dark (LD) cycle. Here, we assessed the circadian phenotype of male STOP KO mice by examining wheel-running activity rhythms and EEG/EMG-defined sleep/wake states under both LD and constant darkness (DD) conditions. Wheel-running activity rhythms in KO and wild-type mice were similarly entrained in LD, and had similar free-running periods in DD. The phase delay shift in response to a light pulse given early in the active phase under DD was preserved in KO mice. KO mice had markedly lower activity levels, lower amplitude activity rhythms, less stable activity onsets, and more fragmented activity than wild-type mice in both lighting conditions. KO mice also spent more time awake and less time in rapid eye movement sleep (REMS) and non-REMS (NREMS) in both LD and DD conditions, with the decrease in NREMS concentrated in the active phase. KO mice also showed altered EEG features and higher amplitude rhythms in wake and NREMS (but not REMS) amounts in both lighting conditions, with a longer free-running period in DD, compared to wild-type mice. These results indicate that the STOP null mutation in mice altered the regulation of sleep/wake physiology and activity rhythm expression, but did not grossly disrupt circadian mechanisms.

Statement of Significance

To understand the disruptions of sleep and circadian rhythms that are often experienced by individuals with schizophrenia, we studied the daily rhythms of wheel-running activity and sleep/wake states in the STOP null mouse model of schizophrenia under light/dark cycles and constant darkness. As in individuals with schizophrenia, STOP null mice exhibited less sleep, reduced sleep spindles, and fragmented activity, compared to wild-type controls. In addition, several aspects of circadian rhythms were altered in STOP null mice, although the phase shift response to light was intact. STOP null mice may be a useful animal model for developing therapeutic strategies for improving sleep and circadian rhythm disruptions in people with schizophrenia.

Key words: microtubule-associated protein; MAP6; circadian rhythms; wheel-running activity; EEG/EMG recording; light/dark cycle; constant darkness; light-induced phase shift; activity fragmentation; transgenic mice

Submitted: 11 June, 2020; **Revised:** 14 October, 2020

Introduction

Disturbances in sleep and circadian (~24 h) rhythms are characteristic of many neuropsychiatric illnesses, including schizophrenia [1–8]. The sleep and circadian rhythm abnormalities associated with schizophrenia include increased sleep latency, decreased total sleep amount, and fragmented sleep [9–12], as well as unstable or reduced daily rest/activity rhythms and abnormal synchronization to lighting cycles [13–15]. Moreover, daily rhythms of gene expression in the frontal cortex [16] and the periphery [17] are disrupted in individuals with schizophrenia.

There is growing evidence that dysfunctions of cytoskeletal microtubules are associated with schizophrenia and other neuropsychiatric illnesses [18, 19]. Microtubules are critical for the structural integrity of neurons and various cellular processes including migration, differentiation, transport of vesicles and organelles, and synaptic functions [20]. Many proteins regulate these microtubule functions, and one such protein is stable tubule only polypeptide (STOP; also known as microtubule-associated protein 6 [MAP6]), which stabilizes microtubules in neuronal somata and axons [21–24] and actin filaments in dendritic spines [25]. Thus, STOP plays important roles in lysosomal transport [26], calcium signaling [27], synaptic plasticity [21], olfactory neurogenesis [28], and axonal tract development [29, 30].

STOP null or knockout (KO) mice show cognitive and behavioral impairments that recapitulate a number of symptoms observed in schizophrenia, and these impairments can be partly alleviated by antipsychotic drugs that are used to treat schizophrenia [21, 31, 32]. For example, STOP null mice display disrupted sensorimotor gating (prepulse inhibition) [33], impaired learning and memory performance [21, 32–38], disorganized activity, and deficits in maternal behavior and social interactions [21, 36] (see also Ref. [39]). Currently, little information is available on the sleep and circadian phenotypes of STOP KO mice. Given the prevalence of sleep and circadian rhythm disruptions in individuals with schizophrenia, it is important to determine whether the STOP null mouse model recapitulates these disturbances in sleep and circadian rhythms.

We recently reported time of day-dependent sleep abnormalities in STOP null mice using EEG/EMG recordings [40]. STOP null mice slept less, and had more fragmented sleep and wakefulness, especially in the dark phase of a 12/12 h light/dark (LD) cycle, compared to wild-type (WT) littermates. In addition, the temporal distributions across the LD cycle of wake, non-rapid eye movement sleep (NREMS), and rapid eye movement sleep (REMS) as well as NREMS EEG delta power (an index of sleep intensity) were abnormal in STOP null mice [40]. These findings are broadly consistent with the sleep patterns reported in individuals with schizophrenia under their usual living conditions [9–12]. The mechanisms underlying these sleep abnormalities in STOP null mice are, however, unclear. The time of day-dependent effects can be caused by disruption of the circadian system, or abnormal synchronization to lighting cycles. These possibilities could not be tested in our previous study [40] as the mice were housed under an LD cycle, which could mask impaired circadian control.

To further investigate the sleep and circadian phenotypes of STOP null mice, we conducted two longitudinal experiments using the same STOP null and WT mice. In the first experiment, we examined the daily rhythms of wheel-running activity (a commonly used index for circadian rhythmicity) under a 12/12 h LD cycle for 15 days followed by constant darkness (DD) for 17 days to assess endogenous circadian rhythms. To examine the resetting response of the circadian system to light, we presented a single light pulse early in the subjective night (active phase) under DD. In the second experiment, we examined the daily rhythms of sleep/wake states in STOP null and WT mice by recording EEG/EMG continuously under a 12/12 h LD cycle for 2 days, followed by DD for 5 days.

Methods

Animals

Adult male STOP null mice and WT littermates at 5 months of age on average (range: 3–7 months) at the beginning of the first experiment were used. These mice were bred in-house from heterozygous breeding mice (C57BL/6 genetic background) originally produced by Dr. A. Andrieux [21]. Only males were used in the present study as in our previous study [40]. All animals were initially housed under a standard 12/12 h LD cycle with lights on at 07:00 am [Zeitgeber Time (ZT) 0] in a temperature-controlled (22 ± 2°C) colony room, with ad libitum access to food and water. Animals were genotyped using PCR analyses, as described in our previous study [40].

The body weight of each mouse was recorded on the first day and on the day following the completion of the entire study (including Experiments 1 and 2), and at two time points during Experiment 1.

All animal handling procedures followed the guidelines of the Canadian Council on Animal Care and were approved by the Dalhousie University Committee on Laboratory Animals.

Experiment 1: Wheel-running activity patterns under LD and DD conditions

Experimental design

Mice were singly housed in clear polycarbonate cages (35.3 cm long × 23.6 cm wide × 19.6 cm high), equipped with a 12.7 cm diameter anodized aluminum running wheel (Model 80820, Lafayette Instrument Co., Lafayette, IN, USA), with bedding and nesting materials. Each cage was placed inside an individual cabinet equipped with an incandescent white light (26.9 W) that was controlled by a timer to provide the same 12/12 h LD cycle as in the animal colony room. To aid routine animal care, an incandescent dim red light (25 W) in the experimental room was kept on continuously throughout the experiment (i.e. under both LD and DD conditions). Food and water were available ad libitum. The cages and water bottles were changed once a week at random times of the day. Cohorts of four mice (two WT and two KO mice) were recorded concurrently.

Mice were placed under a 12/12 h LD cycle for 15 days, followed by DD for 17 days. To examine light-induced phase shifts (delays) in wheel-running activity rhythms, on the third day of DD the cabinet light was turned on for 1 h [13, 41, 42] early in the subjective night (at ~circadian time 14). The timing was based on the onset of darkness under LD (ZT12), given that free-running periods shown during the first 3 days of DD were very close to 24 h (Figure 1).

At the end of the experiment, mice were returned to the animal colony to be housed singly under a 12/12 h LD cycle for at least one week before implantation of EEG/EMG electrodes (see below).

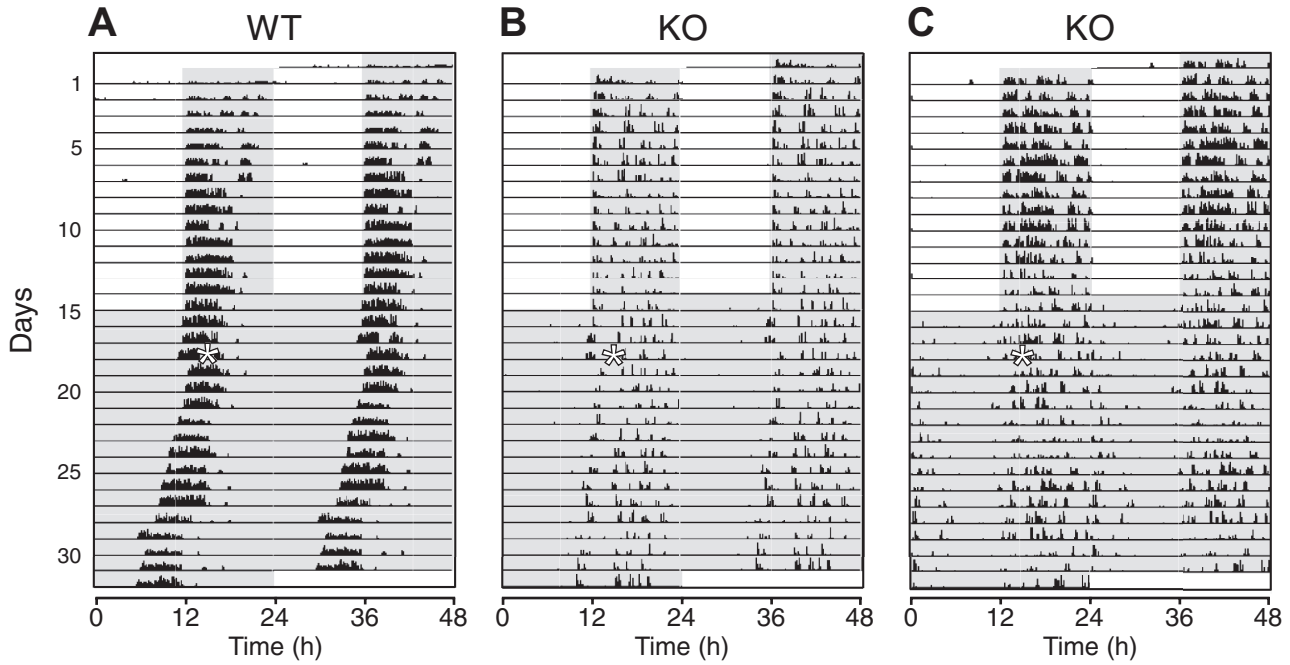

Figure 1. Wheel-running activity in 12/12 h light/dark (LD) and constant darkness (DD) conditions in wild-type (WT) and stable tubule only polypeptide (STOP) knockout (KO) mice. Examples of double-plotted actograms are shown for a WT (A) and two KO (B and C) mice. Wheel-running activity was recorded in an LD cycle for 15 days (days 1–15), followed by DD condition for 17 days (days 16–32). On the third day in DD (day 18), a 1h light pulse (white asterisk on the left of each panel) was given early in the subjective night (active phase), at approximately circadian-time 14. Successive 24 h intervals are plotted from top to bottom (days 1–32) on the left of each panel, and the data are replotted on the right, offset upward by 1 day to provide continuous 48 h records of activity. Vertical black bars on each line represent 10 min bins of wheel-running activity, with the height of the bars corresponding to the number of wheel rotations. The scales for panels (B) and (C) were set to lower maximum values than for panel (A) to improve visualization of the lower activity levels of the KO mice. The gray shading indicates lights-off intervals (in both LD and DD).

Data acquisition and analysis

Wheel-running activity was recorded continuously in 10 min bins using the AWM software (Lafayette Instrument Co.). Actograms were generated using the ActogramJ plugin of ImageJ (NIH, Bethesda, MD, USA).

We analyzed the following activity parameters: daily pattern of activity (distance traveled in m/10 min bin) over the last 7 or 8 days in LD, and the daily total activity (distance traveled in km/day) over the last 7 or 8 days in both LD and DD. The total distance traveled in DD was calculated over a circadian cycle after correcting for the free-running (endogenous) period (tau) in each animal. The subjective night in DD was defined as the half of a circadian cycle from CT12 to CT24, with CT12 determined by fitting a line visually through the activity onsets over the last 7 or 8 days of DD.

The day-to-day variability in the onset of activity under LD (a measure of the precision of daily rhythms under LD) was defined as the standard deviation of daily activity onsets [43] relative to the start of the light phase over the last 7 or 8 days of LD. Activity onset was defined as the start of the first 10 min bin in which activity was greater than or equal to 10% of peak daily activity and followed by one out of the next two bins having at least 10% of peak activity. The results of applying this criterion were similar to those from fitting a line to onset times visually.

The free-running period of the activity rhythm was measured over the last 7 or 8 days of DD using the chi-square periodogram (ImageJ). To estimate the robustness of daily activity rhythms under LD and DD, the periodogram amplitude was measured as the value in arbitrary units (au) at the top of the periodogram curve (Q_p value) [43, 44] in both lighting conditions.

The amplitudes of daily activity rhythms were calculated over the last 7 or 8 days in both LD and DD using a cosinor analysis [45] (https://cosinor.online/app/cosinor.php [46]).

The number of activity bouts per day was counted over the last 7 or 8 days in both LD and DD. An activity bout was defined as a period of activity (>1 wheel rotation) lasting 10 min or longer that was preceded by a period of no activity for 10 min or longer. The number of activity bouts in DD was obtained over a circadian cycle after correcting for each animal's period. The mean duration (min) of each bout and the mean distance traveled (km) per bout were also calculated.

To quantify the phase-shifting response to light pulses, a regression line was fitted by eye through the activity onsets over the 3 days of DD prior to the light pulse, and then extrapolated to the first day after the light pulse. Another line was drawn through the activity onsets for the 7 or 8 days of DD after the light pulse, excluding the first day after the light pulse [47]. The phase shift was measured as the time difference (h) between the projected onsets on the first day after the light pulse as extrapolated from these fitted lines. All analyses were conducted blindly with respect to genotypes.

Experiment 2: Sleep/wake patterns under LD and DD conditions

Implantation of EEG and EMG electrodes

To record sleep/wake states, mice were surgically implanted with EEG/EMG electrodes under 1–2% isoflurane anesthesia as described previously [40]. For EEG recordings, two stainless steel screws were implanted epidurally, one above the frontal cortex (1 mm rostral to bregma, 1 mm to the right of the midline) and

the second above the parietal cortex (2.5 mm caudal to bregma, 1 mm to the left of the midline). A third screw was placed over the cerebellum for grounding and a fourth screw was placed over the parietal cortex contralaterally to the parietal EEG screw for additional anchoring. For EMG recordings, two fluorocarbon-coated, stainless steel wires were inserted into the nuchal muscles. All electrodes were connected to a small plastic connector (Plastics One, Roanoke, VA, USA), which was secured to the skull with dental cement. After surgery, mice were given s.c. injections of an analgesic (Anafen, 5 mg/kg) and an antibiotic (Baytril, 2.5 mg/kg), and an i.p. injection of warm sterile lactated Ringer's (1 mL). The antibiotic was also administered for 1 week via drinking water (45.4 mg/250 mL bottle of drinking water).

Experimental design

Seven to 10 days following surgery, each mouse was placed in a clear Plexiglas cage (38 cm long × 30 cm wide × 30 cm high; no running wheels), with bedding and nesting materials. The cage was placed inside an individual recording chamber equipped with an incandescent white light (26.9 W) controlled by a timer to provide the same 12/12 h LD cycle as in the animal colony room and as in Experiment 1. In the experimental room, an incandescent dim red light (25 W) was kept on continuously to aid animal care, as in Experiment 1. Food and water were available ad libitum. The next day, mice were briefly anesthetized (2%–4% isofluorane) and connected to lightweight recording cables. After 7–11 additional days of habituation, EEG and EMG were recorded continuously for 2 days under LD, followed by 5 days under DD.

Data acquisition and analyses

EEG and EMG signals were amplified (×5,000), band-pass filtered (EEG, 0.1–100 Hz; EMG, 10–100 Hz), digitized (sampling rate at 256 Hz), and stored in a computer using SleepSign software (Kissei Comtec, Irvine, CA, USA). Recordings were automatically scored offline (SleepSign) in 10 s epochs, with each epoch classified as wake (low voltage, high frequency EEG; moderate to high amplitude EMG), NREMS (high voltage, low frequency EEG; low amplitude EMG), or REMS (low voltage, high frequency EEG; very low amplitude EMG indicating atonia, with sporadic spikes indicative of muscle twitches). The automatic scoring was visually inspected and corrected when appropriate, blindly with respect to genotype.

The following parameters were calculated in both LD and DD. The amounts (min) of wake, NREMS, and REMS were calculated in 2, 12, and 24 h intervals in LD or corresponding circadian-time intervals in DD after correcting for each animal's period. The number of episodes (lasting 10 s or longer) and mean duration of episodes for wake, NREMS, and REMS were calculated in 12 h intervals in LD or over each half of a circadian cycle in DD.

EEG power spectra during wake, NREMS, and REMS were computed in 0.5 Hz bins between 0.5 and 50 Hz using a fast Fourier transform (FFT; Hanning window, 2 s). To account for interindividual variability caused by differences in absolute EEG power between animals, the EEG power values were normalized and expressed as a percentage of the total EEG power (0.5–50 Hz) over all three behavioral states, as in our previous study [40] and examined in 12 h intervals in LD or the subjective day and night halves of a circadian cycle in DD. The relative contribution of each sleep or wake state to the total power was weighted in each animal, as in our previous study [40].

We also examined the daily patterns of relative power values in the delta band in the NREMS EEG. Power values were averaged over a 10 s epoch, and the mean value at 2 h intervals in LD or corresponding circadian-time intervals in DD was normalized to the 48 h LD average level in each animal. Epochs containing recording artifacts were visually identified and excluded from the EEG spectral analyses.

The free-running periods of sleep/wake rhythms were measured using the chi-square periodogram analysis (ImageJ), which was applied to wake amounts [48] in 10 min bins over the 5 days of DD. The onset of the subjective day (= circadian time 0) for the first circadian cycle was set at 07:00 am (i.e. the beginning of the light phase in the previous LD cycle).

The amplitude of daily sleep/wake rhythms was obtained using two methods: peak-to-trough amplitude calculation [49] and cosinor analysis [50]. The daily peak-to-trough amplitude (min) for each behavioral state was determined by calculating the difference between the maximum and minimum values over 2 h intervals for each 24 h period in LD, or over corresponding circadian-time intervals for each circadian period in DD, and averaging the maximum–minimum difference across the 2 days of LD or 5 days of DD.

To determine daily amplitudes using cosinor analysis (https://cosinor.online/app/cosinor.php [46]), the amount of each behavioral state was averaged in 2 h intervals over the 2 days of LD, or corresponding circadian-time intervals over the 5 days of DD.

Statistical analyses

Statistical analyses were conducted using Statview 5.0 (SAS Institute Inc., Cary, NC, USA) and IBM SPSS Statistics 21.0 (IBM Corp., Armonk, N.Y., USA) software. Comparisons between WT and STOP null mice were conducted using unpaired, two-tailed t-tests, or Bonferroni post hoc tests following two-way repeated-measures analysis of variance (ANOVA). When required, a logarithmic transformation was used to normalize the data and stabilize the variance. p values <0.05 were considered statistically significant.

Results

Statistics and p values are reported in Supplementary Table S1. Body weights are reported in Supplementary Tables S2 and S3.

Experiment 1: Wheel-running activity patterns under LD and DD conditions

One KO mouse died unexpectedly early during the experiment; thus, a total of 14 WT and 13 STOP KO mice were included in the analyses for the LD condition. The analyses for the DD condition were based on 13 WT and 12 KO mice, after excluding one WT mouse due to development of unusual and irregular activity, and another KO mouse due to technical problems. Activity measures were averaged over the last 7 or 8 days of LD and DD. Examples of actograms throughout the experiment in representative animals of the two genotypes are shown in Figure 1.

Wheel-running activity in all WT and KO mice was robustly entrained to the LD cycle, with activity occurring mainly during the daily dark phase (~97% of the total daily activity amount in both genotypes; Figures 1 and 2A). Activity rhythms persisted

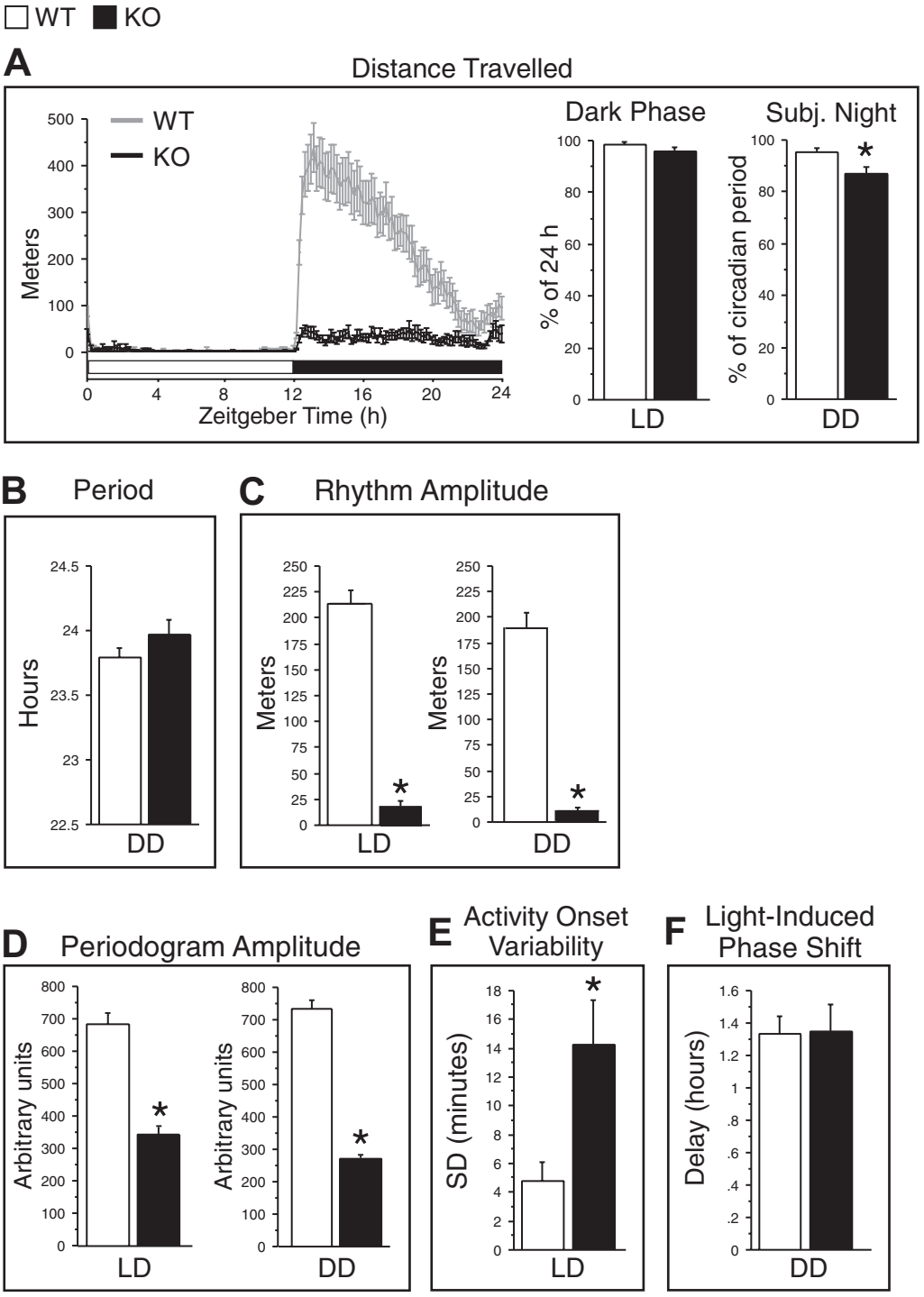

Figure 2. Daily patterns of wheel-running activity in WT (gray lines or white bars) and KO (black lines or bars) mice in 12/12 h light/dark (LD) and constant darkness (DD) conditions. (A) *Left*: The group profiles of distance traveled over the 24 h LD cycle. The time of day is indicated as Zeitgeber Time (ZT), with ZT12 corresponding to the onset of the dark phase. The white horizontal bar indicates the light period and the black bar indicates the dark period. *Right*: The distance traveled in the 12 h dark phase in LD, expressed as a percentage of total 24 h activity, and in the subjective night in DD, expressed as a percentage of the total activity over a circadian cycle (*right*). (B) The free-running period of wheel-running activity rhythms, using the chi-square periodogram, in DD. (C) The amplitude of daily wheel-running activity rhythms, as measured by a cosinor analysis, in LD and DD. (D) Periodogram amplitude, as measured by chi-squared periodogram analysis, in LD and DD (a lower amplitude indicates reduced rhythm stability). (E) Day-to-day variability of onsets (minutes) of wheel-running activity, expressed as the standard deviation (SD) of activity onsets (a greater SD indicates a lower precision of activity onsets). (F) The magnitude of phase delays (hours) to a 1 h light pulse given at approximately circadian-time 14 in DD. Activity measures were averaged in each animal over the last 7 or 8 days of LD (days 8–15) or DD (days 25–32), after wheel-running had stabilized, and then averaged across all animals in each genotype. Data are shown as means + SEM. LD condition: WT, $n = 14$; KO, $n = 13$. DD condition: WT, $n = 11$ or 13; KO, $n = 8$ or 12 (see Results for the explanation of reduced n's in DD) $^*p < 0.05$ versus WT (two-tailed, unpaired t-tests).

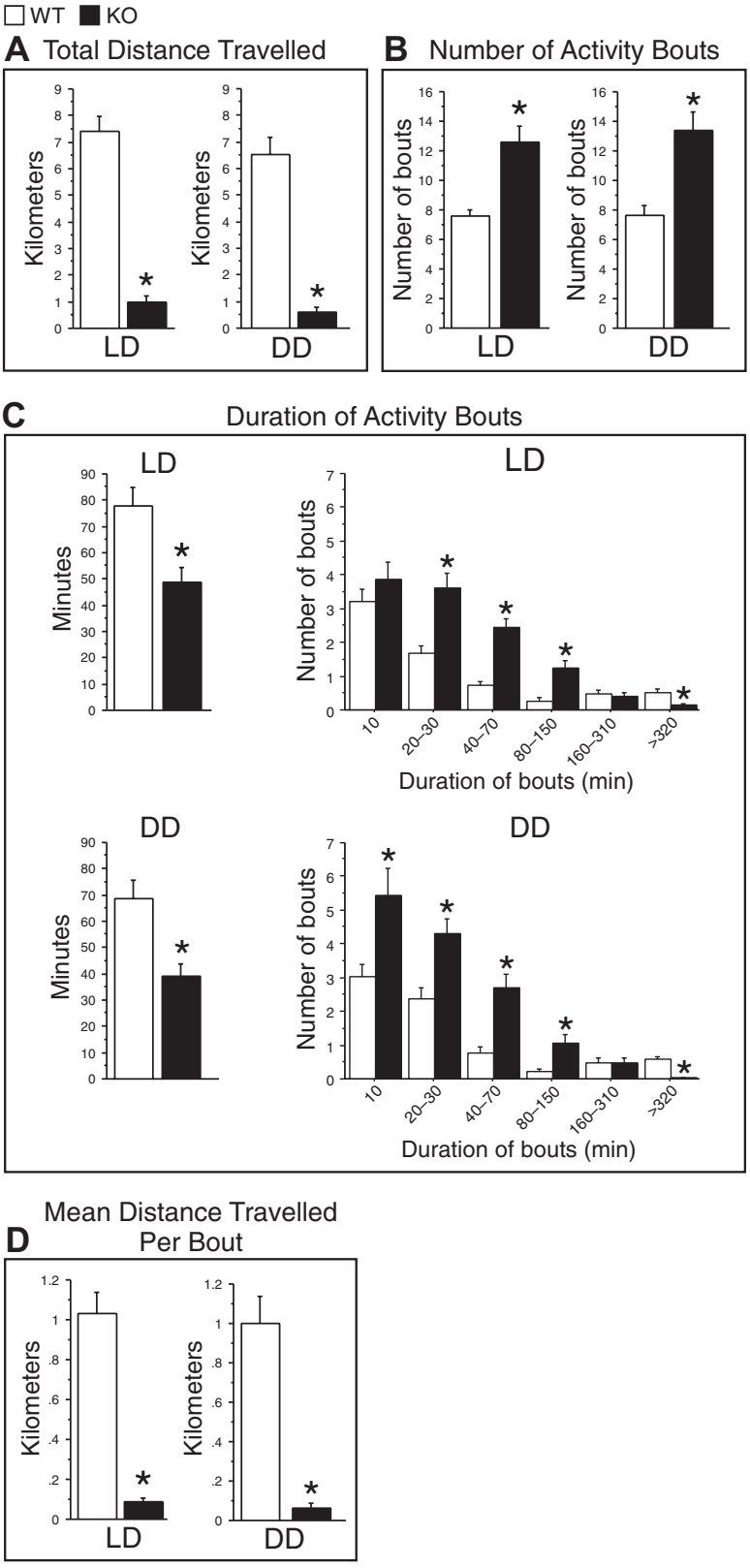

Figure 3. Distance traveled in 12/12 h light/dark (LD) and constant darkness (DD) conditions in WT (white bars) and KO (black bars) mice. (A) The total distance traveled over the 24 h LD cycle and over a circadian cycle in DD. (B) The total number of activity bouts in LD and DD. (C) Mean duration of activity bouts (*left*) and frequency histograms (*right*) of activity bouts as a function of bout duration in LD and DD. All activity bouts were sorted into six consecutive bins of logarithmically increasing duration. (D) Mean distance traveled per activity bout in LD and DD. Activity measures were averaged in each animal over the last 7 or 8 days of LD or DD (see Figure 1) and then averaged over all animals in each genotype. Data are shown as means + SEM. LD condition: WT, $n = 14$; KO, $n = 13$. DD condition: WT, $n = 13$; KO, $n = 12$. $^*p < 0.05$ versus WT (two-tailed, unpaired *t*-tests, except Bonferroni post hoc *t*-tests for (B), *right*).

in DD in both genotypes (Figure 1). However, while all WT mice maintained robust and relatively stable circadian rhythms of activity under DD (e.g. Figure 1A), circadian rhythms in KO mice were much more variable, ranging from relatively stable (e.g. Figure 1B) to less coherent rhythms (e.g. Figure 1C). The proportion of activity occurring during the subjective night under DD was significantly lower in KO than WT mice (Figure 2A, *right*). On average, free-running activity periods were slightly shorter than 24 h in both WT (23.79 ± 0.07 h) and KO mice (23.97 ± 0.11 h), with no significant genotype differences (Figure 2B).

Three parameters of daily activity rhythms differed between genotypes in LD, and the genotype differences persisted under DD. Specifically, the amplitude of daily activity rhythms was much lower in KO than WT mice in both LD (–91%) and DD (–95%; Figure 2C). Likewise, the periodogram amplitude was reduced in KO mice in both LD (–51%) and DD (–63%; Figure 2D and Supplementary Figure S1), indicating reduced rhythm robustness under both lighting conditions in KO mice. In addition, the variability of the onset of daily activity was greater in KO than WT mice (Figure 2E), reflecting reduced precision of rhythm entrainment under LD in KO mice.

Total daily activity (indexed by distance traveled) was reduced by ~90% in both LD and DD in KO mice compared to WT mice (Figure 3A). In addition, activity patterns were severely fragmented in KO mice, characterized by more frequent (Figure 3B) and shorter (Figure 3C, *left*) activity bouts that covered a shorter distance (Figure 3D) under both lighting conditions.

To further examine the ability of KO mice to maintain periods of activity during LD and DD, we calculated the frequency distribution of bout durations. KO mice generated more short and mid-length bouts (10/20–150 min) and fewer long bouts (>320 min) than WT mice under both lighting conditions (Figure 3C, *right*).

Light-induced phase shifts

To assess the phase-shifting effect of light, on the third day in DD mice were exposed to a 1 h light pulse at approximately circadian time 14, a time when light is expected to cause a phase delay [51]. After excluding four mice that showed large (>3 h) phase shifts in activity onset under DD prior to the light pulse, three mice due to technical problems, and one mouse in which activity onsets were too imprecise to assess, phase-shifts were analyzed in 11 WT and 8 KO mice.

As shown in Figure 2F, the light pulse induced phase delays in activity rhythms in both WT (1.33 ± 0.11 h) and KO mice (1.35 ± 0.17 h), with no significant genotype difference.

Experiment 2: Sleep/wake patterns under LD and DD conditions

Five mice were not included in this study because of poor recovery from surgery, illness, or technical problems with EEG recordings, thus leaving 12 WT and 12 KO mice in the analyses of sleep/wake parameters for both LD and DD conditions. For the FFT analyses of the EEG, one WT and one KO mouse were excluded due to EEG signal deterioration over time (although the signal was adequate for sleep/wake parameter analyses), leaving 11 WT and 11 KO mice. Sleep/wake parameters were averaged over 2 days of LD and 5 days of DD.

Consistent with their wheel-running activity rhythms (Experiment 1), the sleep/wake states of all WT and KO mice were robustly entrained to the LD cycle, with more sleep occurring during the daily light phase in both genotypes (Figures 4A–C and 5). Both genotypes maintained circadian sleep/wake rhythms over the 5 days of DD (Figure 4A–C). Similarly to wheel-running activity rhythms, free-running sleep/wake periods were slightly shorter than 24 h in both KO (23.82 ± 0.09 h) and WT mice (23.50 ± 0.12 h; Figure 6A). In contrast to activity rhythms for which there was a weak trend toward longer periods in KO as compared to WT mice (experiment 1), free-running sleep/wake periods were significantly longer in KO than WT mice (Figure 6A).

Daily peak-to-trough amplitudes were significantly greater in KO than WT mice for wake (Figure 6B) and NREMS amounts (Figure 6C) in both LD and DD conditions. However, no significant genotype difference was found for REMS rhythm amplitude in either condition (Figure 6D). Similar results were obtained when circadian amplitudes were determined using cosinor analyses (Supplementary Figure S4A–C).

In general, there were genotype differences in sleep/wake state parameters under LD, and similar genotype differences were observed under DD. Thus, wake amounts were higher in KO than WT mice in both LD (+11% over 24 h) and DD (+15% over a circadian cycle; Figure 5A). Both NREMS (Figure 5B) and REMS amounts (Figure 5C) were reduced in LD and DD in KO relative to WT mice.

The genotype differences for wake and REMS amounts occurred during both the inactive and active phases in both lighting conditions (Figure 5A and C, respectively). Significant differences between genotypes were found for NREMS amounts only during the dark phase in LD and subjective night in DD (Figure 5B).

The changes in sleep and wake amounts in KO mice were associated with changes in sleep architecture. The increase in wake amounts in KO mice was accompanied by a trend toward longer wake episodes in LD and significantly longer episodes in DD (Supplementary Figure S2B). The decrease in NREMS amounts in KO mice was associated with a tendency for shorter NREMS episodes in both lighting conditions (Supplementary Figure S2D). Unlike NREMS, reduced REMS amounts in KO mice were accompanied by significantly less frequent REMS episodes in DD (Supplmentary Figure S2E) and shorter REMS episodes in LD and DD (Supplementary Figure S2F).

To further examine the ability of KO mice to maintain sleep and wake in LD and DD, we calculated the frequency distribution of episode durations, as in our previous study [40]. KO mice generated more mid-length (80–1270 s) and long (>1280 s) wake episodes than WT mice in DD, with a similar trend in LD (Supplementary Figure S3A). Despite their increased frequency, these long wake episodes accounted for a smaller proportion of the total time spent awake in KO than WT mice during the active phase in both lighting conditions (inserts in Supplementary Figure S3A). In addition, KO mice generated fewer long REMS episodes (>80 s), which accounted for a smaller proportion of the total time spent in REMS, compared to WT mice in both LD and DD (Supplementary Figure S3C). No significant genotype differences were found for the frequency of NREMS episodes of any duration in either lighting condition (Supplementary Figure S3B).

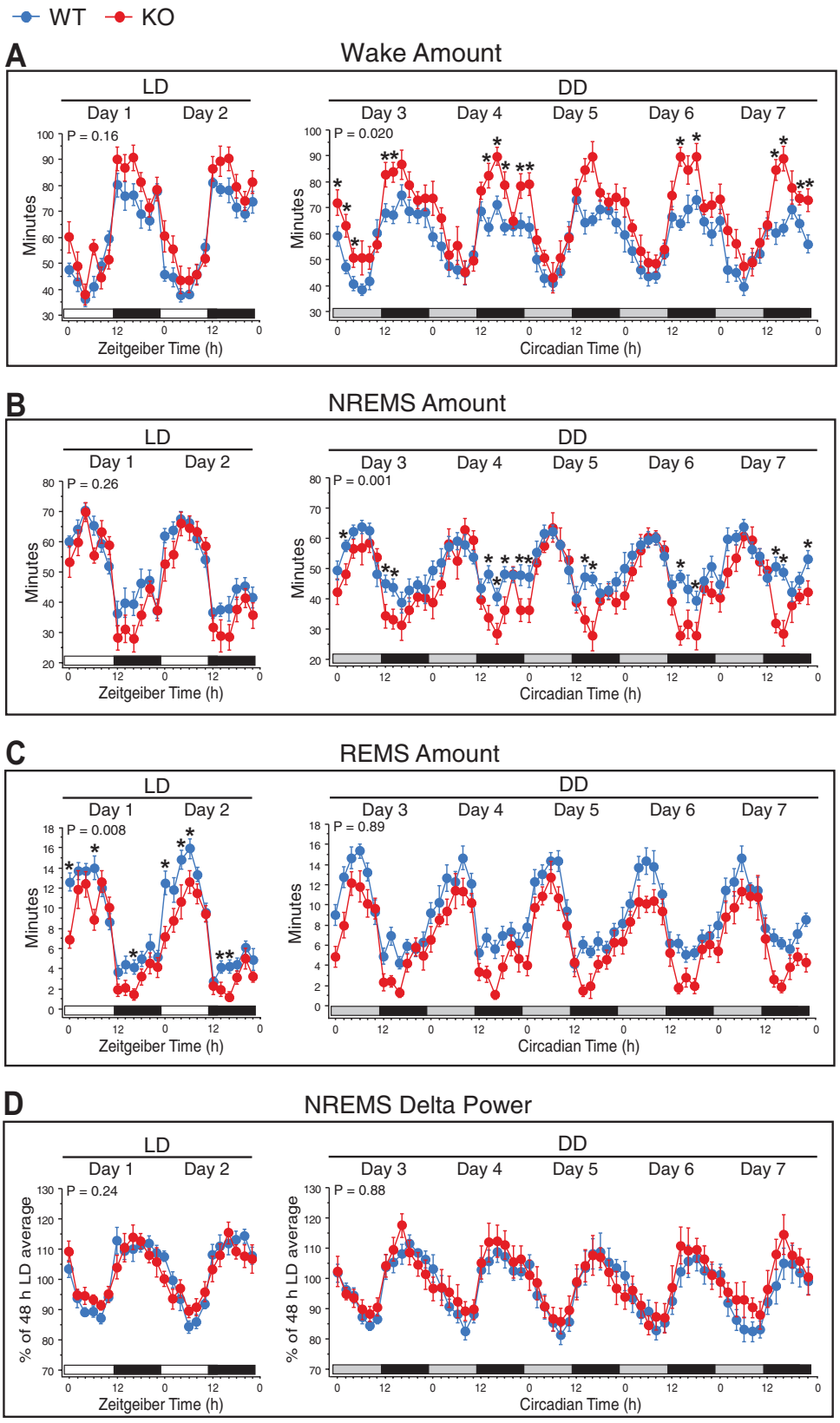

Figure 4. Daily sleep/wake rhythms in 12/12 h light/dark (LD) and constant darkness (DD) conditions in WT (blue circles) and KO (red circles) mice. Time courses of the amounts (minutes) of wake (A), non-rapid eye movement sleep (NREMS: B), and rapid eye movement sleep (REMS: C), and normalized NREMS electroencephalogram (EEG) delta (0.5–4 Hz) power (D) in 2 h intervals across the 2 days of LD (*left*) and 12 circadian-time intervals across the 5 days of DD (*right*). White horizontal bars indicate the light periods in LD, black bars indicate the dark periods in LD or subjective nights in DD, and gray bars indicate the subjective days in DD. Under DD, the time of day is indicated as Circadian Time (CT), with CT12 corresponding to the onset of the subjective night. In (D), EEG power was normalized to the 48 h average in LD. Data are shown as means ± SEM. WT, $n = 12$ (except $n = 11$ in D). KO, $n = 12$ (except $n = 11$ in D). The p values for Genotype × Time interactions are indicated at the top left of each panel. $^{*}p < 0.05$ versus WT (Bonferroni post hoc t-tests after significant Genotype × Time interactions in repeated ANOVAs).

EEG parameters

We examined relative EEG power values (% of all-state total power) in each sleep and wake state, as in our previous study [40]. In general, genotype differences in EEG spectra were observed in wake and REMS in DD and not in LD. Specifically, KO mice showed a greater relative power in slow and intermediate frequency ranges in both wake and REMS EEGs under DD (Figure 7A and C, *right*), while there were no significant genotype differences in NREMS EEG under either DD or LD (Figure 7B).

Three additional EEG parameters were examined, as in our previous study [40]. First, the ratio of power in high-to-low theta frequency bands (7–9 Hz/5–7 Hz) during wakefulness, which is a measure of cortical activation [52, 53], was significantly reduced in KO mice under both LD and DD (Figure 8A), suggesting reduced EEG arousal levels in KO mice in both lighting conditions despite increased wake amounts (see above). Second, delta power (0.5–4 Hz) in the NREMS EEG (% of total power in NREMS), which is a commonly used measure of sleep intensity or homeostatic sleep need [54], did not differ significantly between genotypes in either LD or DD (Figure 8B), nor were there significant genotype differences in the amplitude of NREMS delta power rhythms (% of 48 h LD average level) for either lighting condition (Figures 4D and Supplementary Figure S4D). Third, NREM sleep spindles, which have been suggested to play a role in sleep-dependent memory consolidation [55], were examined by analyzing the relative power (% of total power in NREMS) in the sigma band (10–12 Hz), which corresponds to the frequency of sleep spindles in mice [56]. Sigma power during NREMS was significantly reduced in the subjective day in DD, and there was a trend toward a decrease in the light phase in LD in KO mice (Figure 8C).

Discussion

We found that STOP null mice differed from WT mice in their daily rhythms of wheel-running activity and sleep/wake states under both LD and DD conditions. Specifically, based on wheel-running activity, KO mice had a lower daily rhythm amplitude than WT mice under both lighting conditions. Their average free-running circadian period did not differ significantly from that of WT mice, and the light-induced phase delay response was preserved. EEG recordings showed that the amplitude of daily rhythms in wake and NREMS amounts in STOP null mice was *greater* than in WT mice under both LD and DD conditions, contrary to the results with wheel-running activity rhythms. Their free-running sleep/wake circadian periods were also longer than those in WT mice. These results suggest that the basic features of the circadian system in STOP null mice are essentially intact but that the circadian control of wakefulness and NREMS is altered in the absence of a functional STOP protein.

Altered circadian wheel-running activity patterns in STOP null mice

STOP null mice synchronized their wheel-running activity rhythms to an LD cycle, although their activity levels were generally low, with the amplitude of their rhythms at only about 10% that of WT mice. When released into DD, WT mice maintained the same activity rhythm amplitude, while STOP null mice showed a further amplitude decrease from the LD condition. These results indicate that the LD cycle reinforced the daily rhythms of KO mice, perhaps by exerting masking effects on their activity. In addition, STOP null mice showed greater heterogeneity than WT mice in the stability of circadian activity rhythms under DD, ranging from relatively stable (e.g. Figure 1B) to less coherent rhythms (e.g. Figure 1C). Similarly, heterogeneity in circadian rhythm stability has been reported among individuals with schizophrenia [14, 15].

The free-running period of activity under DD was similar in STOP null and WT mice. This result suggests that circadian clock mechanisms are intact in STOP null mice. Similarly, no change in free-running activity period under DD was reported in several mouse models related to schizophrenia; *blind-drunk* [13] and Sandy [57] null mice, mice lacking Group II metabotropic glutamate receptors 2 and 3 [58] or *Pallidin* [59], and mice expressing human Disrupted in Schizophrenia 1 (DISC1) [60]. Although activity levels can influence the free-running activity period through locomotor activity feedback to the suprachiasmatic nucleus [61], in the present study the genotype differences in levels of activity did not appear to affect circadian timing in these mice.

STOP null mice responded normally with phase delays to a light pulse presented early in the subjective night under DD and showed stable entrainment to LD cycles, despite more variable activity onset at the beginning of the dark phase than in WT mice. Although these results address only some aspects of circadian organization and light responsiveness, they suggest that STOP null mice have intact circadian systems. Together, these results suggest that the differences in sleep organization in KO and WT mice (present study and our previous study [40]) are not a direct consequence of differences in their core circadian clock mechanisms or photic input pathways.

Reduced and fragmented wheel-running activity in STOP KO mice

While rhythmicity was intact, the amount of wheel-running activity was strongly reduced in STOP null mice compared to WT mice in both LD and DD. Furthermore, compared to WT mice, STOP null mice initiated more but shorter activity bouts, resulting in more fragmented activity patterns. Similar findings of reduced and fragmented wheel-running activity in both LD and DD have been reported for other mouse models related to schizophrenia [13, 58–60]. There are several possible explanations for the reduced wheel-running activity of STOP null mice, including lower arousal levels during wake than WT mice (present study), impaired muscle function or motor coordination [30, 33, 62], and potentially reduced motivation for wheel-running, which is naturally rewarding for most rodents [63].

Contrary to our findings, STOP null mice in LD cycles were hyperactive when activity was measured by interruption of infrared light beams [21, 31, 33, 64]. It is possible that the STOP null mice in this study showed other kinds of activity when they were not running in wheels.

Altered sleep architecture and EEG parameters in STOP null mice

STOP null mice had lower amounts of NREMS and REMS under both LD and DD conditions. The difference from WT mice in NREMS amounts was especially marked during the active phase

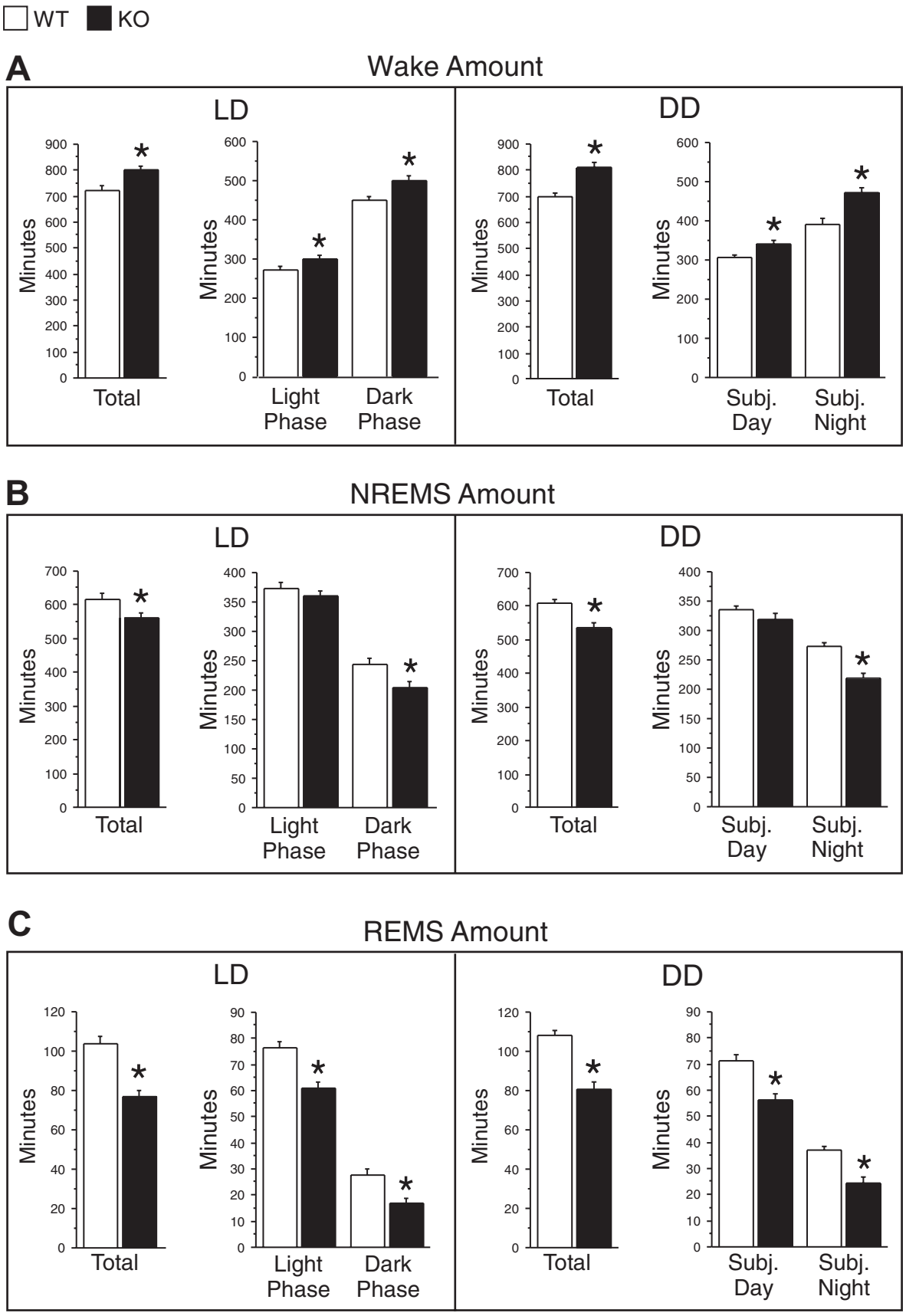

Figure 5. Durations (minutes) of wake (A), NREMS (B), and REMS (C) in WT (white bars) and KO (black bars) mice under 12/12 h light/dark (LD, *left*) and constant darkness (DD, *right*) conditions. LD: amounts for the full 24 h period and for the 12 h light and 12 h dark phases. DD: amounts for the full circadian cycle and for the subjective day and night of a circadian cycle. Data (means + SEM) were based on two successive 24 h periods in LD and five successive circadian cycles in DD (see Figure 4) and averaged for 12 h in LD or one-half of a circadian cycle in DD in each animal. WT, $n = 12$; KO, $n = 12$. *$p < 0.05$ versus WT (two-tailed, unpaired *t*-tests).

under both lighting conditions and was associated with a trend toward shorter NREMS episodes. REMS amounts in KO mice were lower than in WT mice during both the inactive and active phases under both LD and DD. This reduction was reflected in less frequent REMS episodes under DD and shorter REMS episodes under LD and DD, suggesting a reduced capacity or need to initiate, and especially to maintain, REMS. Overall, the alterations in sleep/wake in STOP null mice under LD were similar under DD, indicating that they were not related to abnormalities in photic entrainment or masking effects of light.

STOP KO mice showed more relative EEG power than WT mice for low and intermediate frequency bands during both wakefulness and REMS under DD but not LD. The significance of this finding is unclear. Despite these alterations, the EEG spectra profiles that are characteristic of each state were maintained in KO mice in both lighting conditions, suggesting that the observed changes in sleep/wake amounts were not a result of distorted patterns of cortical EEG activity that could impact behavioral state criteria.

We confirmed our previous finding [40] that STOP null mice slept less under LD than WT mice, which is consistent with behavioral observations of reduced sleep in STOP null mice [21]. Increased nocturnal activity, implying reduced sleep, has also been observed under LD and DD in the *Egr3* mouse model of schizophrenia using piezoelectric monitoring of gross motor activity [65]. Reduction in sleep defined by EEG [60] or immobility [58, 59] has also been found under LD in other mouse models related to schizophrenia. In addition, we confirmed a reduction in both the ratio of power in high-to-low theta frequency bands during waking and sigma power during NREMS in STOP null mice under LD [40]. These results suggest that, despite consistently longer durations of wake and reduced amounts of sleep under both lighting conditions, EEG features associated with greater arousal are diminished in KO mice relative to WT mice.

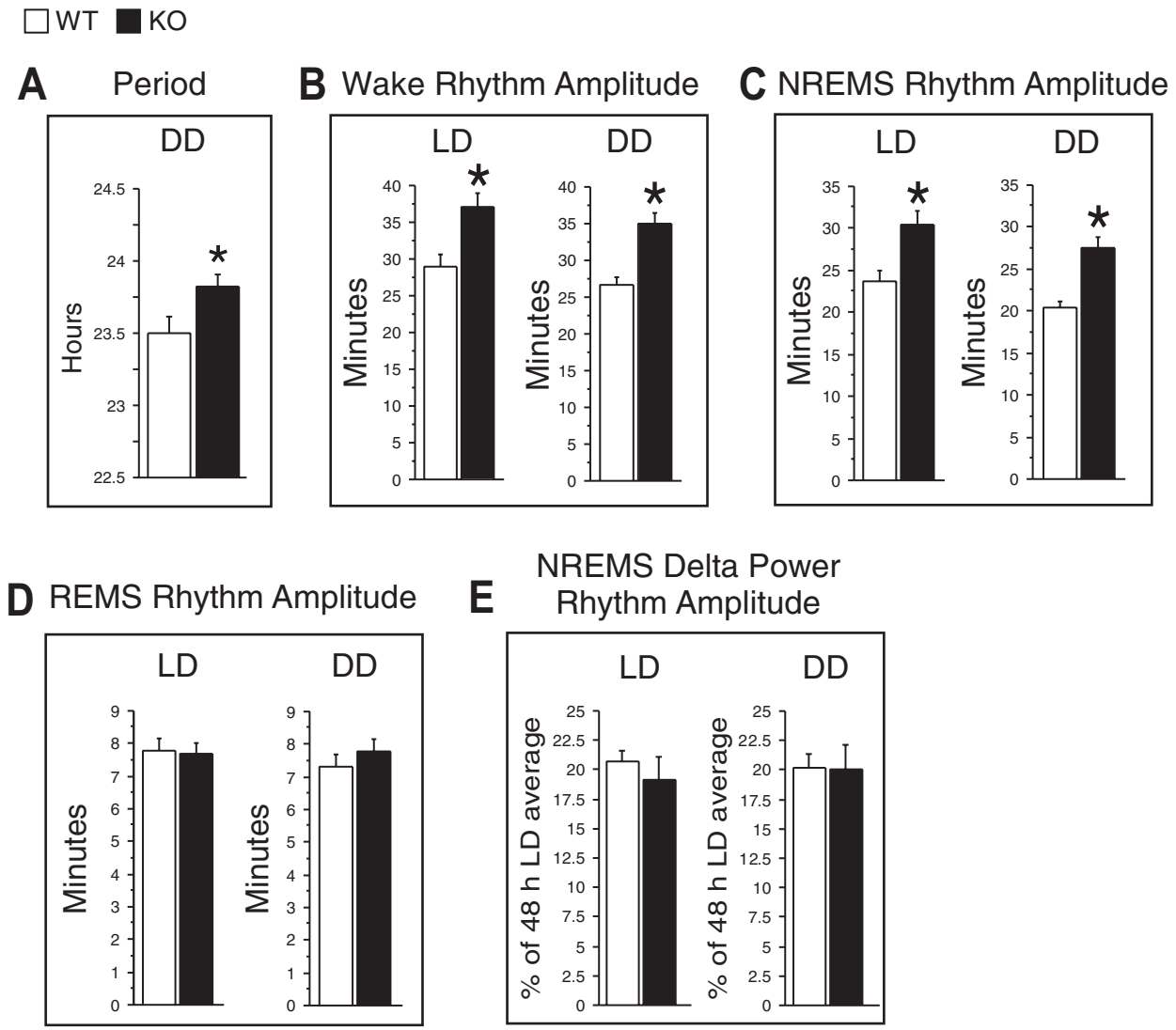

Figure 6. The free-running period of sleep/wake rhythms (A) and the peak-to-trough amplitude of daily rhythms for wake (B), NREMS (C), and REMS (D) amounts, and NREMS EEG delta power (E) averaged over the 2 days of LD and the 5 days of DD in WT (white bars) and KO (black bars) mice. The free-running period was measured using the chi-square periodogram based on profiles of time spent in wakefulness across the 5 days of DD. EEG power was normalized to the 48 h average in LD. Data are shown as means ± SEM. WT, $n = 12$ (except $n = 11$ in E). KO, $n = 12$ (except $n = 11$ in E). *$p < 0.05$ versus WT (two-tailed, unpaired *t*-tests).

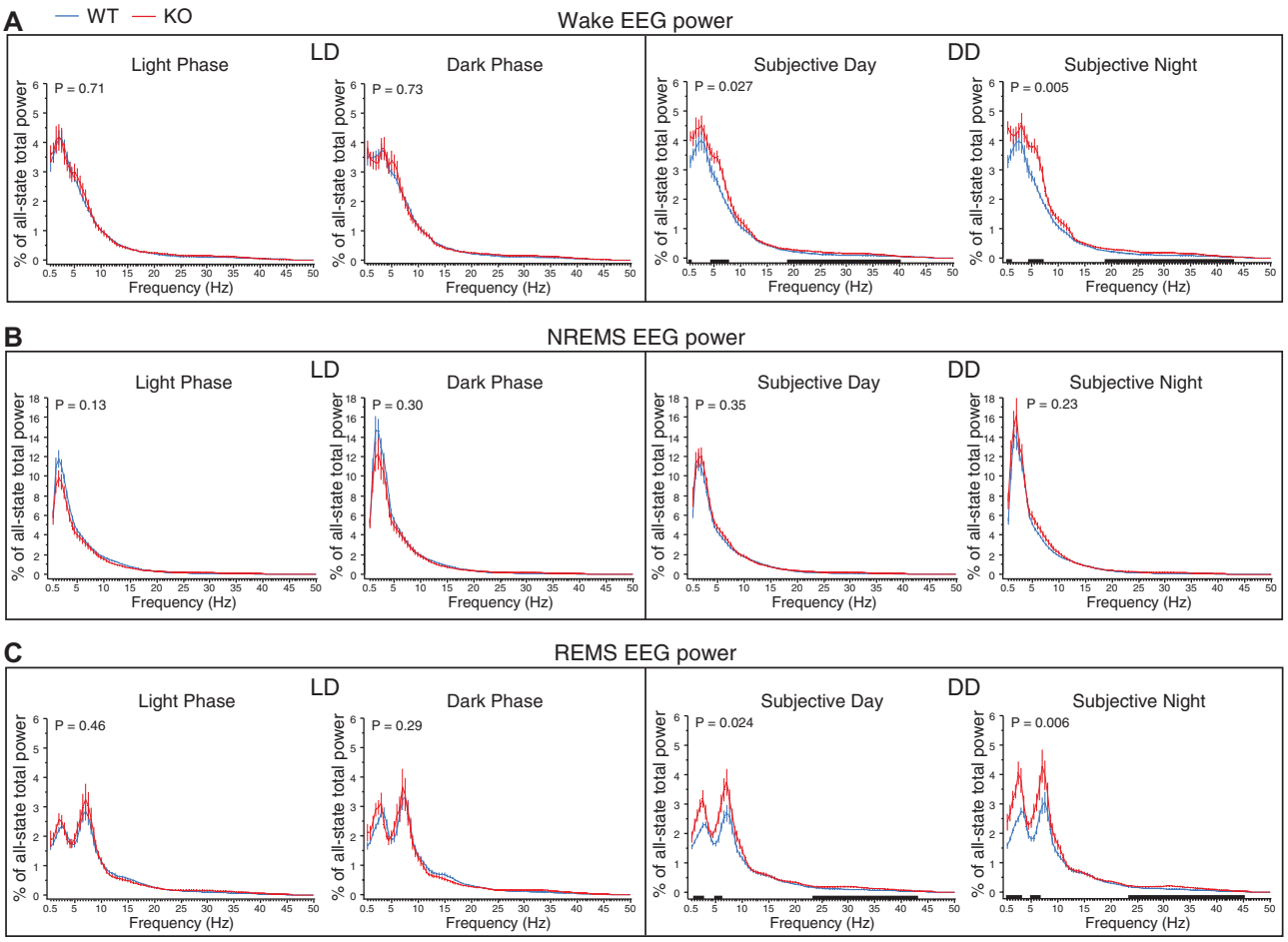

Figure 7. Relative EEG power spectra in wake (A), NREMS (B), and REMS (C) during the 12 h light and 12 h dark phases averaged over the 2 days of LD (*left*) and the subjective day and night averaged over the 5 days of DD (*right*) in WT (blue lines) and KO (red lines) mice (n = 11/genotype). EEG power was normalized to total EEG power (0.5–50 Hz) over all sleep/wake states in each animal, and the mean values (±SEM) were plotted in 0.5 Hz bins. The relative contribution of each behavioral state to total power was weighted in each animal. The p values for Genotype × Bin interactions are indicated at the top left of each panel. Black bars along the X-axis indicate intervals for which EEG power differed significantly between the two genotypes ($p < 0.05$ versus WT, Bonferroni post hoc t-tests). For wakefulness, significant genotype differences were found for 0.5, 4.5–7.5, and 19–40 Hz during the subjective day, and for 0.5–1, 4.5–7, and 19–43 Hz during the subjective night. For REMS, significant genotype differences were found for 1–2.5, 5–6, and 23.5–43 Hz during the subjective day, and for 0.5–3, 5–6.5, and 23.5–45 Hz during the subjective night.

The sleep/wake state and EEG parameters in WT and STOP null mice under LD in the present study were generally within the ranges reported in our previous study [40]. In contrast to our previous study, however, we did not find higher numbers of wake and NREMS episodes in KO than WT mice, perhaps because the WT mice in this study showed twice as many wake and NREMS episodes as in our previous study [40]. The reason for this difference is unknown but may be related to the fact that the mice in this study were older (starting at 18–34 weeks, as opposed to 12–16 weeks, of age) or were exposed to constant dim red light throughout the study.

The neural mechanisms underlying sleep/wake and EEG abnormalities in STOP null mice may include previously reported abnormalities in neurotransmitter systems and synaptic plasticity that are also found in patients with schizophrenia [66, 67]. For example, glutamatergic [21, 68], dopaminergic [31], noradrenergic and serotonergic [69], and cholinergic [34] systems are altered in STOP null mice, and many of these transmitter systems help promote wakefulness [70]. The dopaminergic system, in particular, is thought to be hyperactive in STOP null mice [31, 71], and this could increase wake amounts in these mice. The other neurotransmitter systems are deficient in STOP null mice [21, 31, 34, 68, 69]. How this would lead to increased wake is unclear. However, both noradrenergic and serotonergic systems are known to provide inhibitory inputs to wake-promoting orexin (hypocretin)-containing neurons [72, 73]. Thus, the reduction of this inhibition could contribute to the increased wake in STOP null mice. These mice also show defects in synaptic plasticity [21, 32], and this could alter sleep and EEG patterns. Further studies are needed to clarify any link between the neurochemical and synaptic plasticity abnormalities and sleep and EEG abnormalities in STOP null mice.

Altered circadian sleep/wake patterns in STOP null mice

Circadian free-running periods were similar in both genotypes when assessed using wheel-running activity, but KO mice had significantly longer periods when measured using sleep EEG recordings. The lack of genotype difference based on wheel-running activity might reflect feedback effects of wheel-running activity on circadian periods [74–76], or measurement error

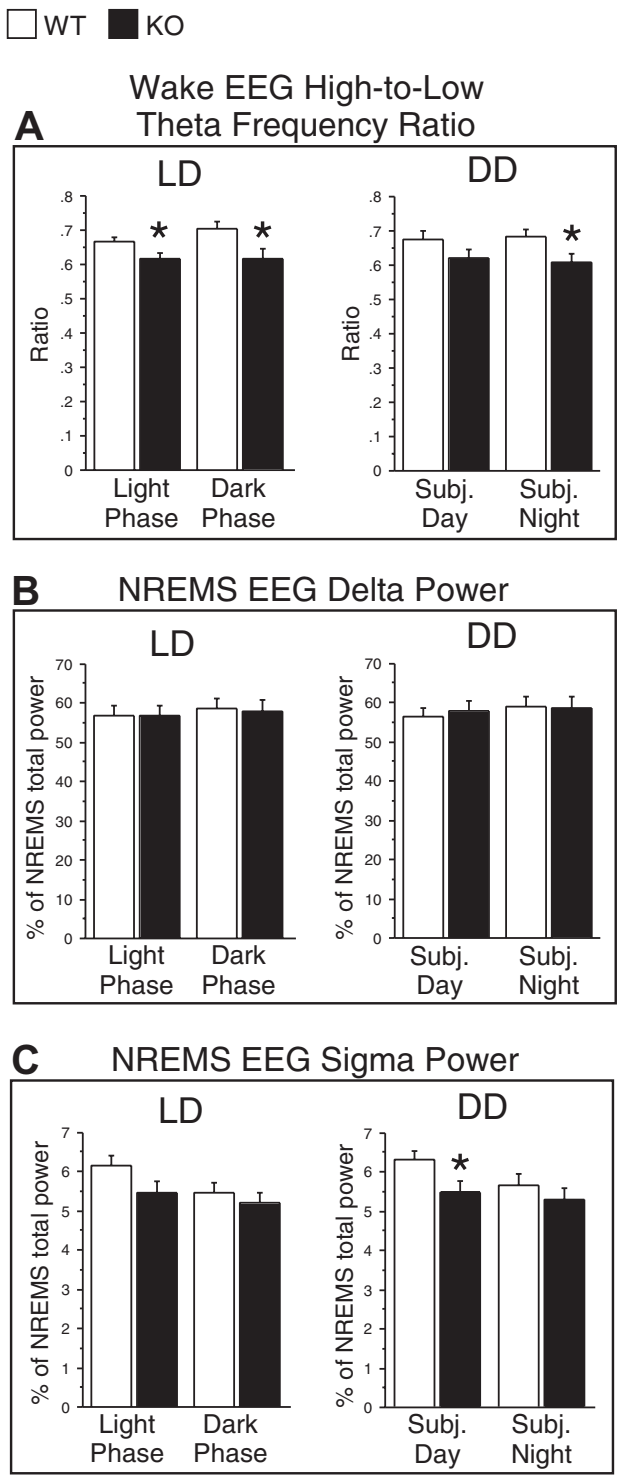

Figure 8. The ratio of power in high-to-low theta frequency bands (7–9 Hz/5–7 Hz) during wakefulness (A), and normalized EEG delta (0.5–4 Hz; B) and sigma (10–12 Hz; C) power during NREMS in the 12 h light and 12 h dark phases in light/dark (LD) conditions and during the subjective day and night in constant darkness (DD) conditions in WT (white bars) and KO (black bars) mice. The EEG power values in the delta and sigma bands were expressed as a percentage of the total EEG power (0.5–50 Hz) during NREMS. Data (means + SEM) were based on two successive 24 h periods in LD and five successive circadian cycles in DD and averaged for 12 h in LD or one-half of a circadian cycle in DD in each animal. n = 11/genotype. *p < 0.05 versus WT (two-tailed, unpaired t-tests).

resulting from the sparse running activity of KO mice. In addition, the low amounts of wheel-running by KO mice might have contributed to their reduced activity rhythm amplitudes in both LD and DD, but KO mice had *greater* rhythm amplitudes for wake and NREMS amounts when measured using EEG recordings. The discrepancy in the direction of change in daily rhythm amplitude may be related to the use of the different methods to assay circadian function (wheel-running activity vs. sleep EEG recordings). Since mice did not have access to an activity wheel during sleep EEG recordings, we cannot assess whether this discrepancy was related to wheel availability. The genotype differences in daily rhythm amplitude based on EEG recording appear to be driven by longer wake durations and shorter NREMS durations in KO than WT mice during their active phases in both lighting conditions, but not during rest phases (see Figures 4A and B and 5A and B).

Thus, genotype differences in wake and NREMS amounts were circadian-phase dependent. This finding suggests that the STOP null mutation altered either circadian regulation of these variables or how the circadian system interacts with their homeostatic sleep regulation. The fact that REMS amounts were uniformly lower in KO than WT mice across circadian phases (Figures 4C and 5C), suggests that changes in the way homeostatic regulation of different sleep stages interacts with circadian regulation is a more likely explanation.

Methodological limitations

Using wheel-running activity as an assay of circadian function has the advantage of allowing precise estimates of entrainment phase and of phase-shifts in response to external events in DD. However, wheel running also carries limitations related to the possible impacts of the STOP null mutation on arousal, motivation, and motor function. In addition, wheel running itself can influence sleep and its circadian expression [74–76]. Future studies of gross motor activity would be useful to address these potential confounding factors.

Another limitation on interpretation of these results is that the STOP null mutation is global and present throughout development, so its effects may not be related exclusively to immediate impacts of the mutation on sleep and circadian regulation in adult mice. Genetic and developmental compensatory mechanisms may occur, and there may be differences in maternal care of mutant mice, which could contribute to functional differences as adults.

Conclusions

We characterized circadian patterns of activity and sleep/wake states in the STOP null mouse model of schizophrenia in both LD and DD conditions. Many sleep and circadian abnormalities observed in STOP null mice were consistent with those seen in individuals with schizophrenia, including reduced sleep amounts and NREMS sigma power, reduced activity levels and activity rhythm amplitude, and fragmented activity. STOP null mice might therefore be a useful animal model for studying the link between sleep and circadian disruptions and microtubule dysfunction in neuropsychiatric illnesses and for developing effective pharmacotherapies for these conditions.

Acknowledgments

We thank Janette Nason for mouse breeding and genotyping, Mikaela Friedrich for assistance with analyses of wheel-running activity, Joan Burns for assisting surgery, and Maxine Profitt and Farah Henry for assistance with EEG/EMG scoring. We also thank

Dr. Annie Andrieux for generously providing a breeding trio of STOP null mice used to establish a colony at our university.

Funding

This work was supported by grants from the Dalhousie Department of Psychiatry Research Fund and Canadian Institutes of Health Research (MOP-259183, PJT-159779).

Disclosure Statement

Financial disclosure: None.

Non-financial disclosure: None.

Data Availability

The data underlying this article will be shared on a reasonable request to the corresponding author.

References

1. Chouinard S, *et al*. Sleep in untreated patients with schizophrenia: a meta-analysis. *Schizophr Bull*. 2004;**30**(4):957–967.
2. Wulff K, *et al*. Sleep and circadian rhythm disruption in schizophrenia. *Br J Psychiatry*. 2012;**200**(4):308–316.
3. Cohrs S. Sleep disturbances in patients with schizophrenia: impact and effect of antipsychotics. *CNS Drugs*. 2008;**22**(11):939–962.
4. Monti JM, *et al*. Sleep and circadian rhythm dysregulation in schizophrenia. *Prog Neuropsychopharmacol Biol Psychiatry*. 2013;**43**:209–216.
5. Chan MS, *et al*. Sleep in schizophrenia: a systematic review and meta-analysis of polysomnographic findings in case-control studies. *Sleep Med Rev*. 2017;**32**:69–84.
6. Winsky-Sommerer R, *et al*. Disturbances of sleep quality, timing and structure and their relationship with other neuropsychiatric symptoms in Alzheimer's disease and schizophrenia: insights from studies in patient populations and animal models. *Neurosci Biobehav Rev*. 2019;**97**:112–137.
7. Kaskie RE, *et al*. Sleep disturbances in schizophrenia: what we know, what still needs to be done. *Curr Opin Psychol*. 2020;**34**:68–71.
8. Ashton A, *et al*. Disrupted sleep and circadian rhythms in schizophrenia and their interaction with dopamine signaling. *Front Neurosci*. 2020;**14**:636.
9. Lauer CJ, *et al*. Sleep in schizophrenia: a polysomnographic study on drug-naive patients. *Neuropsychopharmacology*. 1997;**16**(1):51–60.
10. Nofzinger EA, *et al*. Electroencephalographic sleep in clinically stable schizophrenic patients: two-weeks versus six-weeks neuroleptic-free. *Biol Psychiatry*. 1993;**33**(11–12):829–835.
11. Ganguli R, *et al*. Electroencephalographic sleep in young, never-medicated schizophrenics. A comparison with delusional and nondelusional depressives and with healthy controls. *Arch Gen Psychiatry*. 1987;**44**(1):36–44.
12. Tandon R, *et al*. Electroencephalographic sleep abnormalities in schizophrenia. Relationship to positive/negative symptoms and prior neuroleptic treatment. *Arch Gen Psychiatry*. 1992;**49**(3):185–194.
13. Oliver PL, *et al*. Disrupted circadian rhythms in a mouse model of schizophrenia. *Curr Biol*. 2012;**22**(4):314–319.
14. Martin J, *et al*. Actigraphic estimates of circadian rhythms and sleep/wake in older schizophrenia patients. *Schizophr Res*. 2001;**47**(1):77–86.
15. Wirz-Justice A, *et al*. Disturbed circadian rest-activity cycles in schizophrenia patients: an effect of drugs? *Schizophr Bull*. 2001;**27**(3):497–502.
16. Seney ML, *et al*. Diurnal rhythms in gene expression in the prefrontal cortex in schizophrenia. *Nat Commun*. 2019;**10**(1):3355.
17. Johansson AS, *et al*. Altered circadian clock gene expression in patients with schizophrenia. *Schizophr Res*. 2016;**174**(1–3):17–23.
18. Marchisella F, *et al*. Microtubule and microtubule associated protein anomalies in psychiatric disease. *Cytoskeleton (Hoboken)*. 2016;**73**(10):596–611.
19. Varidaki A, *et al*. Repositioning microtubule stabilizing drugs for brain disorders. *Front Cell Neurosci*. 2018;**12**:226.
20. Matamoros AJ, *et al*. Microtubules in health and degenerative disease of the nervous system. *Brain Res Bull*. 2016;**126**(Pt 3):217–225.
21. Andrieux A, *et al*. The suppression of brain cold-stable microtubules in mice induces synaptic defects associated with neuroleptic-sensitive behavioral disorders. *Genes Dev*. 2002;**16**(18):2350–2364.
22. Qiang L, *et al*. Tau does not stabilize axonal microtubules but rather enables them to have long labile domains. *Curr Biol*. 2018;**28**(13):2181–2189.e4.
23. Tortosa E, *et al*. Dynamic palmitoylation targets MAP6 to the Axon to promote microtubule stabilization during neuronal polarization. *Neuron*. 2017;**94**(4):809–825.e7.
24. Cuveillier C, *et al*. MAP6 is an intraluminal protein that induces neuronal microtubules to coil. *Sci Adv*. 2020;**6**(14):eaaz4344.
25. Peris L, *et al*. A key function for microtubule-associated-protein 6 in activity-dependent stabilisation of actin filaments in dendritic spines. *Nat Commun*. 2018;**9**(1):3775.
26. Schwenk BM, *et al*. The FTLD risk factor TMEM106B and MAP6 control dendritic trafficking of lysosomes. *EMBO J*. 2014;**33**(5):450–467.
27. Brocard J, *et al*. MAP6 interacts with Tctex1 and Cav 2.2/N-type calcium channels to regulate calcium signalling in neurons. *Eur J Neurosci*. 2017;**46**(11):2754–2767.
28. Benardais K, *et al*. Loss of STOP protein impairs peripheral olfactory neurogenesis. *PLoS One*. 2010;**5**(9):e12753.
29. Deloulme JC, *et al*. Microtubule-associated protein 6 mediates neuronal connectivity through Semaphorin 3E-dependent signalling for axonal growth. *Nat Commun*. 2015;**6**:7246.
30. Gimenez U, *et al*. 3D imaging of the brain morphology and connectivity defects in a model of psychiatric disorders: MAP6-KO mice. *Sci Rep*. 2017;**7**(1):10308.
31. Brun P, *et al*. Dopaminergic transmission in STOP null mice. *J Neurochem*. 2005;**94**(1):63–73.
32. Delotterie D, *et al*. Chronic administration of atypical antipsychotics improves behavioral and synaptic defects of STOP null mice. *Psychopharmacology (Berl)*. 2010;**208**(1):131–141.
33. Fradley RL, *et al*. STOP knockout and NMDA NR1 hypomorphic mice exhibit deficits in sensorimotor gating. *Behav Brain Res*. 2005;**163**(2):257–264.
34. Bouvrais-Veret C, *et al*. Sustained increase of alpha7 nicotinic receptors and choline-induced improvement of

learning deficit in STOP knock-out mice. *Neuropharmacology*. 2007;**52**(8):1691–1700.
35. Powell KJ, *et al*. Cognitive impairments in the STOP null mouse model of schizophrenia. *Behav Neurosci*. 2007;**121**(5):826–835.
36. Bégou M, *et al*. The stop null mice model for schizophrenia displays [corrected] cognitive and social deficits partly alleviated by neuroleptics. *Neuroscience*. 2008;**157**(1):29–39.
37. Kajitani K, *et al*. Nitric oxide synthase mediates the ability of darbepoetin alpha to improve the cognitive performance of STOP null mice. *Neuropsychopharmacology*. 2010;**35**(8):1718–1728.
38. Fournet V, *et al*. Both chronic treatments by epothilone D and fluoxetine increase the short-term memory and differentially alter the mood status of STOP/MAP6 KO mice. *J Neurochem*. 2012;**123**(6):982–996.
39. Faure A, *et al*. Dissociated features of social cognition altered in mouse models of schizophrenia: focus on social dominance and acoustic communication. *Neuropharmacology*. 2019;**159**:107334.
40. Profitt MF, *et al*. Disruptions of sleep/wake patterns in the stable tubule only polypeptide (STOP) null mouse model of schizophrenia. *Schizophr Bull*. 2016;**42**(5):1207–1215.
41. Diessler S, *et al*. Rai1 frees mice from the repression of active wake behaviors by light. *Elife*. 2017;**6**:e23292
42. Timothy JWS, *et al*. Circadian disruptions in the myshkin mouse model of mania are independent of deficits in suprachiasmatic molecular clock function. *Biol Psychiatry*. 2018;**84**(11):827–837.
43. Brown LA, *et al*. Telling the time with a broken clock: quantifying circadian disruption in animal models. *Biology (Basel)*. 2019;**8**(1):18.
44. Sokolove PG, *et al*. The chi square periodogram: its utility for analysis of circadian rhythms. *J Theor Biol*. 1978;**72**(1):131–160.
45. Nelson W, *et al*. Methods for cosinor-rhythmometry. *Chronobiologia*. 1979;**6**(4):305–323.
46. Molcan L. Time distributed data analysis by Cosinor. Online application. *bioRxiv*. 2019;805960. https://www.biorxiv.org/content/10.1101/805960v1
47. Jud C, *et al*. A guideline for analyzing circadian wheel-running behavior in rodents under different lighting conditions. *Biol Proced Online*. 2005;**7**:101–116.
48. Edgar DM, *et al*. Influence of running wheel activity on free-running sleep/wake and drinking circadian rhythms in mice. *Physiol Behav*. 1991;**50**(2):373–378.
49. Franken P, *et al*. The transcription factor DBP affects circadian sleep consolidation and rhythmic EEG activity. *J Neurosci*. 2000;**20**(2):617–625.
50. Easton A, *et al*. The suprachiasmatic nucleus regulates sleep timing and amount in mice. *Sleep*. 2004;**27**(7):1307–1318.
51. Daan S, *et al*. A functional analysis of circadian pacemakers in nocturnal rodents. II. The variability of phase response curves. *J. Comp. Physiol*. 1976;**106**:253–266.
52. Leemburg S, *et al*. Sleep homeostasis in the rat is preserved during chronic sleep restriction. *Proc Natl Acad Sci USA*. 2010;**107**(36):15939–15944.
53. Wigren HK, *et al*. Basal forebrain lactate release and promotion of cortical arousal during prolonged waking is attenuated in aging. *J Neurosci*. 2009;**29**(37):11698–11707.
54. Borbély AA, *et al*. Sleep homeostasis and models of sleep regulation. *J Biol Rhythms*. 1999;**14**(6):557–568.
55. Manoach DS, *et al*. Abnormal sleep spindles, memory consolidation, and schizophrenia. *Annu Rev Clin Psychol*. 2019;**15**:451–479.
56. Kim D, *et al*. Characterization of topographically specific sleep spindles in mice. *Sleep*. 2015;**38**(1):85–96.
57. Bhardwaj SK, *et al*. Constant light uncovers behavioral effects of a mutation in the schizophrenia risk gene Dtnbp1 in mice. *Behav Brain Res*. 2015;**284**:58–68.
58. Pritchett D, *et al*. Deletion of metabotropic glutamate receptors 2 and 3 (mGlu2 & mGlu3) in mice disrupts sleep and wheel-running activity, and increases the sensitivity of the circadian system to light. *PLoS One*. 2015;**10**(5):e0125523.
59. Lee FY, *et al*. Sleep/wake disruption in a mouse model of BLOC-1 deficiency. *Front Neurosci*. 2018;**12**:759.
60. Jaaro-Peled H, *et al*. Abnormal wake/sleep pattern in a novel gain-of-function model of DISC1. *Neurosci Res*. 2016;**112**:63–69.
61. Hughes ATL, *et al*. Feedback actions of locomotor activity to the circadian clock. *Prog Brain Res*. 2012;**199**:305–336.
62. Sébastien M, *et al*. Deletion of the microtubule-associated protein 6 (MAP6) results in skeletal muscle dysfunction. *Skelet Muscle*. 2018;**8**(1):30.
63. Meijer JH, Robbers Y. Wheel running in the wild. *Proc Biol Sci*. 2014;**281**(1786): 20140210.
64. Bégou M, *et al*. Post-pubertal emergence of alterations in locomotor activity in stop null mice. *Synapse*. 2007;**61**(9):689–697.
65. Maple AM, *et al*. Influence of schizophrenia-associated gene egr3 on sleep behavior and circadian rhythms in mice. *J Biol Rhythms*. 2018;**33**(6):662–670.
66. Salavati B, *et al*. Imaging-based neurochemistry in schizophrenia: a systematic review and implications for dysfunctional long-term potentiation. *Schizophr Bull*. 2015;**41**(1):44–56.
67. Soares JC, *et al*. Neurochemical brain imaging investigations of schizophrenia. *Biol Psychiatry*. 1999;**46**(5):600–615.
68. Brenner E, *et al*. Hypoglutamatergic activity in the STOP knockout mouse: a potential model for chronic untreated schizophrenia. *J Neurosci Res*. 2007;**85**(15):3487–3493.
69. Fournet V, *et al*. The deletion of the microtubule-associated STOP protein affects the serotonergic mouse brain network. *J Neurochem*. 2010;**115**(6):1579–1594.
70. Scammell TE, *et al*. Neural circuitry of wakefulness and sleep. *Neuron*. 2017;**93**(4):747–765.
71. Bouvrais-Veret C, *et al*. Microtubule-associated STOP protein deletion triggers restricted changes in dopaminergic neurotransmission. *J Neurochem*. 2008;**104**(3):745–756.
72. Li Y, *et al*. Direct and indirect inhibition by catecholamines of hypocretin/orexin neurons. *J Neurosci*. 2005;**25**(1):173–183.
73. Yamanaka A, *et al*. Orexin neurons are directly and indirectly regulated by catecholamines in a complex manner. *J Neurophysiol*. 2006;**96**(1):284–298.
74. España RA, *et al*. Running promotes wakefulness and increases cataplexy in orexin knockout mice. *Sleep*. 2007;**30**(11):1417–1425.
75. Welsh D, *et al*. Effect of running wheel availability on circadian patterns of sleep and wakefulness in mice. *Physiol Behav*. 1988;**43**(6):771–777.
76. Vyazovskiy VV, *et al*. Running wheel accessibility affects the regional electroencephalogram during sleep in mice. *Cereb Cortex*. 2006;**16**(3):328–336.